



MINISTRY OF AVIATION

AERONAUTICAL RESEARCH COUNCIL

CURRENT PAPERS

The Design and
Development of an Air-Bearing
for the Measurement of Damping
in Yaw on a Jet-Blowing Model

by

A. P. Cox

LONDON: HER MAJESTY'S STATIONERY OFFICE

1965

PRICE 5s 6d NET



C.P. No. 796

April, 1964

THE DESIGN AND DEVELOPMENT OF AN AIR-BEARING FOR THE MEASUREMENT
OF DAMPING IN YAW ON A JET-BLOWING MODEL

by

A. P. Cox

SUMMARY

This Note describes the design and development of an air-bearing support assembly, for damped oscillation measurements of yaw damping derivatives on V./S.T.O.L. blowing models, commencing with a jet-flap model. The bearing, fitted within the fuselage, allowed freedom in yaw, but supported all the other forces and moments. Typically, with a bearing air supply of 0.07 lb/sec at 60 p.s.i.g., a vertical load of 400 lb could be sustained, or a pitching-moment of 650 lb in. with the vertical load reduced to 150 lb. From measurements of the overall rig damping rate, the internal damping of the bearing was determined by allowing for the contributions from spring hysteresis loss and external aerodynamic loads. The internal damping of the bearing, which was unaffected by the transmission of the simulated wing airflow (amounting to 2 lb/sec at 15 p.s.i.g.), was found to be negligible as long as the bearing capacity was not exceeded.

CONTENTS

	<u>Page</u>
1 INTRODUCTION	4
2 DESIGN OF BEARING ASSEMBLY	4
2.1 Specification	4
2.2 Detailed design	5
2.3 Instrumentation	5
2.4 Modifications	6
3 STATIC LOADING TESTS	7
3.1 Procedure	7
3.2 Lift capacity	7
3.3 Pitching-moment and drag capacity	7
3.4 Air consumption	7
4 MEASUREMENT OF OSCILLATORY DAMPING DUE TO BEARING	8
4.1 Technique of measurement	8
4.2 Bearing friction at maximum load	8
4.3 Bearing internal damping - without main air flow	9
4.4 Effect of pressure and flow of jet-blowing air	10
5 FUTURE DEVELOPMENTS	10
SYMBOLS	10
REFERENCES	11

APPENDIX 1 - Measurement of rig damping by the free oscillation technique 12-14

ILLUSTRATIONS - Figs.1-11 -

DETACHABLE ABSTRACT CARDS -

ILLUSTRATIONS

	<u>Fig.</u>
Original bearing design	1
Final bearing design	2
Modified bearing assembly	3
Method of gap measurement for horizontal bearings	4

ILLUSTRATIONS (Cont'd)

	<u>Fig.</u>
Lift capacity of bearing	5
Combined lift and pitching-moment capacity of bearing	6a,b
Effect of lift load on horizontal bearing surface gaps	7a,b
Arrangement for the measurement of internal oscillatory damping	8
A typical trace of oscillatory damping with the bearing overloaded	9
Change in equivalent sliding friction as bearing starts to float	10
Variation of N_{ψ} with spring hysteresis parameter, $T\epsilon^2$	11

1 INTRODUCTION

Although a considerable amount of wind-tunnel model testing has now been completed for S.T.O.L. and V.T.O.L. aircraft employing jet-blowing devices to obtain high lift, this has not included much work on the measurement of dynamic stability derivatives. A programme of model tests has started at R.A.E. to ascertain the adequacy of conventional quasi-static methods of prediction for such configurations. The first experiments, on an existing jet-flap model, concerned the measurement of the yaw-damping derivative, $N_{\dot{\psi}}$, by a free-oscillation technique.

An air connection and model support system was required which permitted the model to yaw freely over an angular range of $\pm 6^\circ$ without affecting, or being affected by, the air supply to the jet-flap wings. This Note describes the design and development of a suitable internal air-bearing support arrangement, including some measurements of the bearing friction and its load and moment capacity. The various problems which arose during development in 1960 have been considered in some detail, to indicate those features which would require attention in any future design. A separate report will be issued on the aerodynamic measurements made on the particular jet-flap model mentioned above.

2 DESIGN OF BEARING ASSEMBLY

The initial decision to use an internal bearing support arrangement (enclosed within the confines of the jet-flap model fuselage) rather than an external bearing, was influenced by various considerations. The additional deflection problem of an external bearing arrangement would probably have introduced design complications. Further, the larger drag and sideforce moments would have involved increases in bearing area and friction. Moreover, since it was likely that internal bearing arrangements would prove necessary for possible future rigs with several degrees of freedom, it was desirable to investigate the associated air distribution problems. Finally, the relatively large fuselage allowed a plausible internal arrangement to be envisaged.

2.1 Specification

As the jet-flap model had already been the subject of extensive balance measurements¹, it was possible to evaluate the maximum nett loads that the bearing assembly would have to withstand. A vertical load capacity of ± 150 lb was necessary to support the possible combinations of aerodynamic lift and model weight. Further, assuming that the horizontal forces and moments were to be taken completely by two bearings, some 7.5 in. apart vertically, as determined by the fuselage size, each of these bearings might be subjected to a maximum load of about 100 lb. The maximum quantity of air that the bearing assembly had to transmit to the wings was about 2 lb/sec, at an exit pressure ratio of 2:1. The model had to be able to yaw through at least $\pm 6^\circ$ without throttling the flow of the jet-blowing air or altering its distribution between the wings. Lastly, provision had to be made for measuring the angle of rotation by means of a suitable transducer to obtain a continuous record of model oscillations.

2.2 Detailed design

A sectional drawing of the bearing, as originally designed, is shown in Fig. 1. The bearing consisted essentially of two plane horizontal and two quasi-cylindrical vertical air-bearing surfaces. All the bearing faces were made as large as available space would allow, and the vertical bearings were placed as far apart as possible to minimise the loads on these bearings arising from the moments applied to the model. As each of these vertical surfaces was required to carry a maximum load of 100 lb, the small upper bearing clearly had to support a much higher maximum load per unit area than the lower one. Tests of an experimental device, consisting of two bearings on a shaft, showed that the upper vertical bearing would have at most a maximum load-carrying capacity of 50 lb at 60 p.s.i.g. However, an estimate* of the load-carrying capacity of the horizontal bearing faces showed that they should be capable of supporting a maximum vertical load of ± 580 lb at 60 p.s.i.g., compared with the required range of only ± 150 lb. It was therefore hoped that this excess capacity might assist in supporting pitching and rolling moments; subsequent tests (see para. 3.3) confirmed that the necessary contribution from the horizontal bearing faces to the moment-carrying capacity was, in fact, obtained.

The quantity of air which could be supplied to the bearings was severely limited by the small space available for connecting supply pipes, so each of the lower bearing faces was restricted to a single row of nozzles. In the case of the horizontal faces, the nozzles were placed as near the outer edge as possible to give the bearing greater stiffness for withstanding moments. To ensure adequate air distribution at small clearances, the nozzles were connected to $1/16$ in. wide V-grooves in the bearing faces. Each nozzle discharged into a separate section of the groove, which was subdivided (using an epoxy resin filling) to enable the bearing to sustain asymmetrical loads. Every air-bearing gap had to be adjustable with the bearing assembled, so the quasi-cylindrical bearings were slightly tapered. Initially, all gaps were set at 0.003 in.

Duralumin was used in the construction of the bearing, to simplify initial manufacture and subsequent modification. However, the duralumin bearing surfaces proved prone to damage, especially if any relative movement of opposing faces occurred in the absence of the air supply to the bearing.

2.3 Instrumentation

An air-spaced, twin-ganged variable capacitor, giving a linear change of capacitance with angle of rotation of 1 pF for 6° , was incorporated in the top of the bearing assembly. The moving vanes were fixed to an insulated spindle which, in the original design was connected to the outer casing of the bearing assembly by means of a phosphor-bronze strip. This strip prevented sideways motion and imposed a small downward load on an air-bearing at the lower end of

*The empirical method of estimation, which was based on the results of earlier tests, enabled a general comparison to be made readily between different bearing configurations. A 25% drop in pressure through the nozzles was assumed, with a linear variation of static pressure in the bearing from the nozzles to the edge of the bearing. The resulting pressure distribution in the bearing face was integrated to give the load-carrying capacity.

the spindle which ensured a smooth motion with complete freedom from sticking. The fixed sets of plates of the twin-ganged capacitor were connected by co-axial cable to the measuring equipment, from which the voltage output, directly proportional to capacitance and hence linearly dependent on the angle of rotation, was fed into a trace recorder.

2.4 Modifications

During preliminary laboratory tests, several modifications were found to be necessary (see Fig.2); Fig.3 shows the bearing assembly prior to its installation in the model.

The bearing, as originally made, floated freely with the central jet-blowing duct at atmospheric pressure. However, pressurisation of this duct caused air to leak asymmetrically down the 0.003 in. gap between the central portions of the inner and outer casings, forming an unstable air-bearing arrangement. Consequently, the outer casing was forced sideways, and the air-bearing assembly jammed. To cure this trouble, grooves were cut around the circumference of the outer casing at intervals, thus avoiding pressure variation around the circumference. Below the lowest groove, which was vented to atmosphere, the 0.003 in. gap was enlarged to 0.030 in.

Considerable difficulty was experienced in measuring gap variations with the bearing under load. Two dial gauges reading to 0.0001 in. were mounted as shown in Fig.4. Gauges A and B indicated variations in the lower and upper gaps respectively of the horizontal bearings. Readings obtained during early tests showed poor repeatability and were difficult to interpret. It was found that the gaps set during assembly could be completely altered by differential movements in the two screw threads of the lower bearing when the bearing was pressurised. In order to improve the repeatability by preloading the threads, the lid of the pressure box was forced upwards by a ring of steel balls bedded on an annulus of P.V.C., and eight clamping plates were added between the two main components of the outer casing. (See Fig.2.) Before this fault was fully appreciated, it was believed erroneously that the bearing was floating with unequal top and bottom gaps. To try to rectify this, the size of the nozzles in the upper horizontal bearing was increased to 3/64 in. However, this change had little apparent effect on bearing performance.

One further deficiency only appeared after considerable use in the wind tunnel. Under conditions of model buffeting, spurious vibrations were indicated by the capacitance measuring equipment. By this time, the bearing had already been stripped down, lapped and reassembled several times following minor damage to the bearing faces and, consequently, the stiffness in pitch and roll was somewhat reduced. Because the lower end of the capacitor spindle was located in the fixed side of the assembly whilst the upper end was connected to the moving side, the spindle tilted when the model vibrated, resulting in capacitance fluctuations. To remedy this behaviour, a ball race was added at the top of the spindle, so that both ends of the spindle were now supported by the fixed part of the bearing. Also, the rotation of the moving part was transferred to the capacitor by a wire link, insensitive to pitch and roll. This modification, although successful, required careful vertical adjustment of the ball race to avoid overloading the small air-bearing supporting the spindle.

3 STATIC LOADING TESTS

3.1 Procedure

After modification, as described in Section 2.4, the bearing assembly was subjected to loading tests. Dial gauges were attached, as shown in Fig.4, and a loading frame was fixed to the outer casing to permit simulation of lift and pitching-moment. Positive lifts were represented by inverting the bearing assembly. The value of air pressure just sufficient to float the loaded assembly could be easily determined by the freedom in yaw*. However, the need to avoid any constraint in yaw made the simulation of drag difficult, and so the combined effect of lift, drag and pitching-moment was not determined directly. Instead, the performance of the bearing assembly was evaluated in terms of the lift and pitching-moment combination equivalent to the worst combination of lift, drag and pitching-moment expected in practice.

3.2 Lift capacity

The variation of minimum floating pressure with positive lift load is shown in Fig.5, together with the corresponding empirical estimate (see footnote to Page 5). The result for negative lift, which are not presented in this Note, were invariably similar to those for positive lift. Variation of the total (top + bottom) gap had little effect on the lift capacity at a given air pressure. With the smallest total gap (0.0035 in.), the variations of bottom gap and total gap with load and pressures are shown in Fig.7; the variations in total gap arose from the remaining flexibility of the bearing structure (see para.2.4).

3.3 Pitching-moment and drag capacity

As the required horizontal force and moment capacity exceeded that of the two quasi-cylindrical bearings alone (see Section 2.2), it was necessary to obtain some contribution from the horizontal bearings. The minimum floating pressure was therefore determined for various combinations of lift and pitching-moment by eccentric loading, with the total (top + bottom) gap progressively reduced from 0.006 in. to 0.005 in. and then to 0.0035 in. (Fig.6). With the latter gap, there was a substantial increase in the moment capacity, indicating a contribution by the horizontal bearings. With this gap setting, which was used throughout the subsequent testing, it was possible to support the maximum required loading (150 lb lift, 650 lb in. moment) at a bearing air pressure of 60 p.s.i.g.

3.4 Air consumption

The mass flow rate of air supplied to the bearing surfaces was measured and found to be 0.07 lb per sec at 60 p.s.i.g., with the bearing in its final form.

*It had originally been hoped to use the electrical resistance across the bearing gaps as a measure of bearing overload. This did not prove feasible during development testing, because electrical contact inexplicably existed across the bearing, although it was floating quite freely. However, the short circuit disappeared during the subsequent wind tunnel tests, allowing the adoption of the electrical technique.

4 MEASUREMENT OF OSCILLATORY DAMPING DUE TO BEARING

The variation of bearing friction near the limit of load-carrying capacity was first determined (para.4.2). Below this limit, the internal damping of the bearing was then assessed from measurements of overall damping, with due allowance for the contributions from the spring hysteresis and the aerodynamic loads on the moving assembly (para.4.3). Some final tests concerned the changes in damping resulting from pressurisation of the central air duct and transmission of jet-blowing air at representative flow rates (para.4.4).

The magnitude of the measured rig damping rates was, in fact, very low. The maximum damping in the rig, attributable mainly to spring hysteresis, amounted to some 3% of the mean value expected in the wind-tunnel tests. Under conditions of minimum rig damping, as much as 12 minutes was needed for the amplitude of oscillation to decay from $\pm \bar{\psi}_0$ to $\pm \bar{\psi}_0/e$, where e represents the usual exponential factor.

4.1 Technique of measurement

The loading frame was replaced by a structure (see Fig.8) which consisted of a discharge pipe for the air representing the flow to the wings of the model, together with a horizontal bar carrying weights to vary the load and moment of inertia of the system. The two pipes connected to the outlet ports on the air-bearing assembly were joined at a point above and on the axis of the bearing so that the air could be discharged vertically upwards along the axis, thus avoiding the generation of torques and moments. The member carrying the weights was stiffened by a length of 2 in. x 1 in. duralumin rectangular bar. The whole of the stationary side of the system was also made as rigid as possible, since even slight flexibility had a marked effect at the low damping rates being measured.

The coil springs regulating the oscillatory motion were connected to the weight bar at various distances apart. Normally the amplitude of oscillation was measured visually by means of a pointer attached to the end of the bar moving over a scale. At higher damping rates; the recording equipment was employed.

The value of the damping derivative, $N_{\dot{\psi}}$ was determined by the free oscillation technique, with observations of the period of oscillation and the decay of amplitude with time from an initial value, $\bar{\psi}_0$. Usually, a value of 6° was chosen for $\bar{\psi}_0$, but a reduced value of 3° was sometimes used due to limitations of spring extension.

4.2 Bearing friction at maximum load

As it was not known whether bearing friction increased gradually or suddenly when the maximum capacity was approached, this was investigated by applying a "negative lift" load and reducing the air supply pressure to the bearing by small increments. At each stage a damping curve was recorded and the equivalent bearing static friction calculated from the expression,

$$Q = - \frac{\pi^2 C}{T} \times \frac{d\bar{\psi}}{dt} \quad , \quad (\text{see Appendix 1}),$$
 where C represents the yawing moment of inertia, and T the period of oscillation.

With a constant value for Q over the amplitude range, $d\bar{\psi}/dt$ also would be constant and damping would occur at a uniform rate. This happened in practice once the bearing friction was appreciable and the associated damping curves (Fig. 9) were thus characteristically different from exponential damping curves obtained with the freely-floating bearing. Because there was a considerable risk of damaging the bearing faces, this test was not extended to overload by a combined lift and pitching-moment. From the results plotted in Fig. 10, it will be seen that for all practical purposes, with lift loading only*, the bearing was either "solid" or completely free.

4.3 Bearing internal damping - without main air flow

The internal damping of the bearing in the freely-floating condition was determined from measurements of the damping rate with the free oscillation technique. Using standard methods (see Appendix 1), the overall damping coefficient, N_{ψ}^* , was calculated from measurements on different spring and inertia combinations, not exceeding the bearing capacity. In order to deduce the internal friction of the bearing, $N_{\psi b}^*$, from the measured overall damping coefficient, allowance had to be made for the spring hysteresis damping, $N_{\psi s}^*$, as well as the aerodynamic damping, $N_{\psi e}^*$, due to the external shape of the rig.

In order to measure the aerodynamic damping due to the external shape of the rig, a lightweight replica of the moving components was mounted inverted on the top of the outlet nozzle. The increase in damping caused by this addition, which represented the external damping of the basic rig, amounted to only about 0.005 lb ft/radian/sec. Moreover, there was no significant variation with the position of the dummy weights. To assess the damping contribution due to spring hysteresis, $N_{\psi s}^*$, it was assumed that the springs only released a proportion, ϕ , of their stored energy in each half cycle. The damping of the ensuing motion would be exponential (see Appendix 1), with $N_{\psi s}^* \propto Tl^2$ for a given pair of springs. As the variation of $N_{\psi e}^*$ with weight position was negligible, the contribution of spring hysteresis was directly obtained by variation of the moment of inertia with the springs at a fixed spring spacing (see Fig. 11). The expected linear variation of N_{ψ}^* with Tl^2 was obtained. However the value of $\partial(N_{\psi}^*)/\partial(Tl^2)$ increased when the springs were closely spaced, which could have resulted from variations in the overall system stiffness. At each spring spacing, however, the extrapolated value of N_{ψ}^* as $Tl^2 \rightarrow 0$ amounted to about -0.005 lb ft/rad. sec. Since this was fully accounted for by the measured external damping, $N_{\psi e}^*$, it was therefore concluded that the internal damping of the bearing, $N_{\psi b}^*$ was negligible.

*In practice, the wind-tunnel tests sometimes showed a more gradual increase in friction as the limiting capacity was approached. Particularly with a large moment load, the presence of static friction could not always be readily detected from the appearance of the damping curves. The measurement of a virtually infinite electrical resistance was found to be a more reliable indication that a metallic air-bearing was floating completely freely.

4.4 Effect of pressure and flow of jet-blowing air

By sealing off the outlet nozzle, it was possible to pressurise the central air duct in the bearing assembly. With this pressure set at 15 p.s.i.g., the damping rate was measured. The outlet was unsealed and the experiment was repeated with 2 lb/sec of air passing through the bearing at the same pressure. It was found that there was no measurable effect on damping in either case. Moreover, the static pressure in one limb of the exit pipe stayed at a steady value, showing that oscillation did not alter the flow distribution between the two bearing outlets.

5 FUTURE DEVELOPMENTS

While the yaw bearing proved reasonably satisfactory, its use was limited to the measurement of one derivative on a particular model, and its moment-carrying capacity was only just sufficient to cope with experimental requirements. For a more versatile bearing, it would be advantageous to avoid supporting moments within the confines of the model. For instance, some form of spherical bearing might well be used, giving freedom about any desired axis, although the problem of how to apply the required constraints would have to be solved.

The use of duralumin, although convenient, proved rather unsatisfactory because the bearing was so easily damaged by contact between opposing surfaces. As an alternative to metallic machined bearings, it would be worth investigating newer constructional methods such as the use of electro-deposition or epoxy-resins particularly in view of the possibility of forming one surface on another.

SYMBOLS

a_0	initial amplitude of spring
a_n	amplitude of spring after (n) cycles
C	total yawing moment of inertia of rig (slugs ft ²)
k	total spring stiffness (lb ft/radian)
K	stiffness of one spring (lb/in.)
ℓ	moment arm of each spring (ft)
L	lift applied to bearing (lb)
M	pitching-moment applied to bearing (lb/in.)

SYMBOLS (Cont'd)

n	number of oscillations in (t) secs
N	yawing-moment (lb ft)
$N_{\dot{\psi}}^*$	$\partial N / \partial \dot{\psi}$ ($N_{\dot{\psi}}^* = N_{\dot{\psi}s}^* + N_{\dot{\psi}e}^* + N_{\dot{\psi}b}^*$)
$N_{\dot{\psi}b}^*$	internal bearing damping contribution to $N_{\dot{\psi}}^*$
$N_{\dot{\psi}e}^*$	external rig damping contribution to $N_{\dot{\psi}}^*$
$N_{\dot{\psi}s}^*$	spring hysteresis damping contribution to $N_{\dot{\psi}}^*$
P_o	bearing-air supply pressure (p.s.i.g.)
Q	sliding friction of bearing (lb ft)
t	time for amplitude to decrease from $\bar{\psi}_o$ to $\bar{\psi}$
t_d	time for amplitude to decrease from $\bar{\psi}_o$ to $\bar{\psi}_o/e$
T	period of oscillation
ϕ	ratio of energy released by spring after one half cycle
ψ	angle of yaw (generally the amplitude of oscillation)
$\bar{\psi}_o$	initial amplitude of oscillation
$\bar{\psi}$	amplitude of oscillation after (t) secs.

REFERENCES

<u>No.</u>	<u>Author</u>	<u>Title, etc.</u>
1	Butler, S.F.J. Guyett, M.B. Moy, B.A.	Six-component low-speed tunnel tests of jet-flap complete models with variation of aspect-ratio, dihedral, and sweepback, including the influence of ground proximity. R.A.E. Report No. Aero 2652, A.R.C.23432, June, 1961.
2	Lessing, H.C. Fryer, T.B. Mead, M.H.	A system for measuring the dynamic lateral stability derivatives in high-speed wind tunnels. N.A.C.A. T.N.3348, A.R.C. 24578, December, 1954.

APPENDIX 1

MEASUREMENT OF RIG DAMPING BY THE FREE OSCILLATION TECHNIQUE

(a) Basic equations

Providing the load-carrying capacity of the bearing is not exceeded, so that it is floating freely, the normal type of oscillatory motion ensues with exponential decay of peak amplitude from the initial amplitude, $\bar{\psi}_0$. Thus

$$\psi(t) = \bar{\psi}_0 e^{(N_{\psi} \cdot t/2C)} \cos(2\pi t/T) \quad (1)$$

with the peak amplitude envelope defined by

$$\bar{\psi}(t) = \bar{\psi}_0 e^{(N_{\psi} \cdot t/2C)} \quad (2)$$

If t_d is the time for the peak amplitude of oscillation to decay from $\bar{\psi}_0$ to $\bar{\psi}_0/e$ then, by (2),

$$N_{\psi} = -(2C/t_d) \quad (3)$$

(It can also be shown that t_d is also the decay time at which $\bar{\psi}$ is most sensitive to small changes in N_{ψ} .)

The time period of oscillation is given by

$$T = 2\pi \sqrt{C/k} \quad (4)$$

where,

C is the moment of inertia

and

k is the spring moment stiffness

For a given pair of springs, each at a distance l (ft) from the centre of rotation, and each having stiffness K (lb/in.),

$$\text{then } k = 24 K l^2 \text{ (lb ft/radian)} \quad (5)$$

$$\text{and hence, } C = k T^2 / 4\pi^2 = 0.6075 K T^2 l^2 \text{ slugs ft}^2 \quad (6)$$

(b) Spring hysteresis damping

During each half-cycle of the oscillatory motion, there is a variation in the spring energy proportional to the square of the amplitude, a_0 . If a constant fraction $(1 - \phi)$ of this energy is dissipated in each half-cycle, the available energy is reduced by a factor ϕ , with a corresponding reduction of $\phi^{1/2}$ in the amplitude of the motion.

After n cycles,

$$a_n = a_0 \phi^n \quad (7)$$

but

$$t = n T \quad (8)$$

so that

$$\begin{aligned} a_n &= a_0 \phi^{(t/T)} \\ &= a_0 e^{(t/T) \log_e \phi} \end{aligned} \quad (9)$$

Comparing (2) with (9), we can define an equivalent spring hysteresis damping coefficient, $N_{\psi S}$, where

$$(N_{\psi S} \cdot t)/2C = t \cdot \log_e(\phi)/T$$

i.e.

$$N_{\psi S} = (2C/T) \log_e(\phi) \quad (10)$$

so that from (6)

$$N_{\psi S} = 1.215 K T \ell^2 \log_e(\phi) \quad (11)$$

Thus, with a given pair of springs, $N_{\psi S} \propto T \ell^2$ and $N_{\psi S} \rightarrow 0$ as $T \rightarrow 0^*$

(c) Bearing static friction in overloaded condition

Consider a more general oscillatory motion,

$$\psi = \bar{\psi}(t) \cos(2\pi/T) \quad (12)$$

where $\bar{\psi}(t)$ again defines the peak amplitude envelope. At the completion of each cycle when $\psi(t) = \bar{\psi}(t)$, all the energy is contained by the springs, and this energy is of the form

$$E = \text{constant} + k \bar{\psi}^2/2 \quad (13)$$

Thus, in a particular cycle, the decrease in energy is given by

$$\delta E \simeq k \bar{\psi} \delta \bar{\psi} \quad (14)$$

but

$$\delta \bar{\psi} \simeq (d\bar{\psi}/dt) \cdot T \quad (15)$$

and using (6)

$$\delta E \simeq - (4\pi^2 C/T) \cdot \bar{\psi}(t) \cdot (d\bar{\psi}/dt) \quad (16)$$

Let Q be the frictional torque, assumed constant. During each cycle, the total angular movement is $4 \cdot \bar{\psi}(t)$ and the energy dissipation is therefore equal to $4Q \cdot \bar{\psi}(t)$. By comparison with (16), it follows that

*In practice, ϕ is amplitude dependent², so that $N_{\psi S}$ is generally of the form, $N_{\psi S} = T(a + b\psi)$. However, in the present case, damping due to spring hysteresis was sufficiently close to logarithmic for this effect to be ignored.

$$4Q \cdot \bar{\psi}(t) = - (4\pi^2 C/T) \cdot \bar{\psi}(t) \cdot (d\bar{\psi}/dt)$$

i.e.

$$Q = - (\pi^2 C/T) \cdot (d\bar{\psi}/dt)$$

With the constant value for Q, this implies linear, rather than exponential, damping of the oscillatory motion.

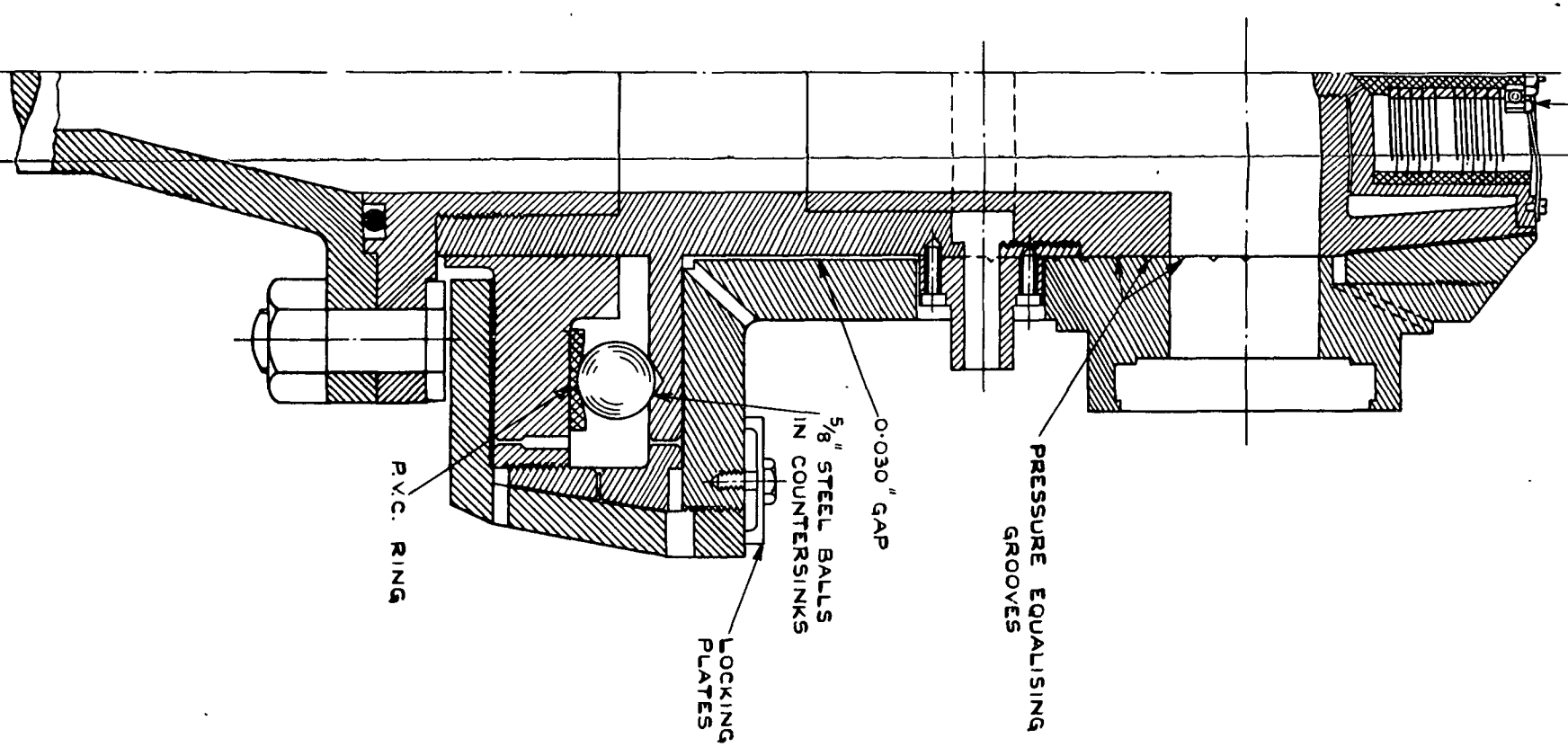
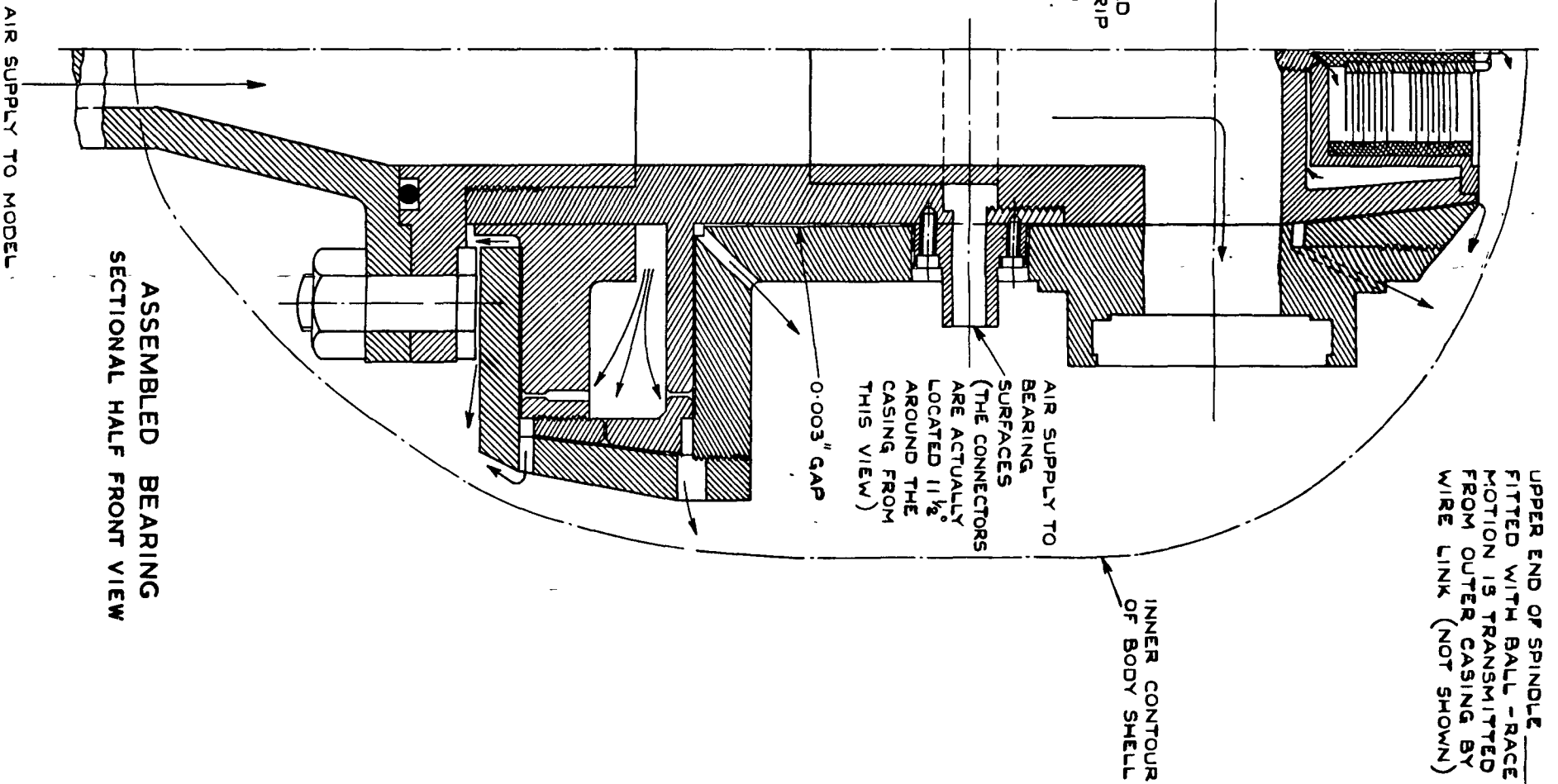
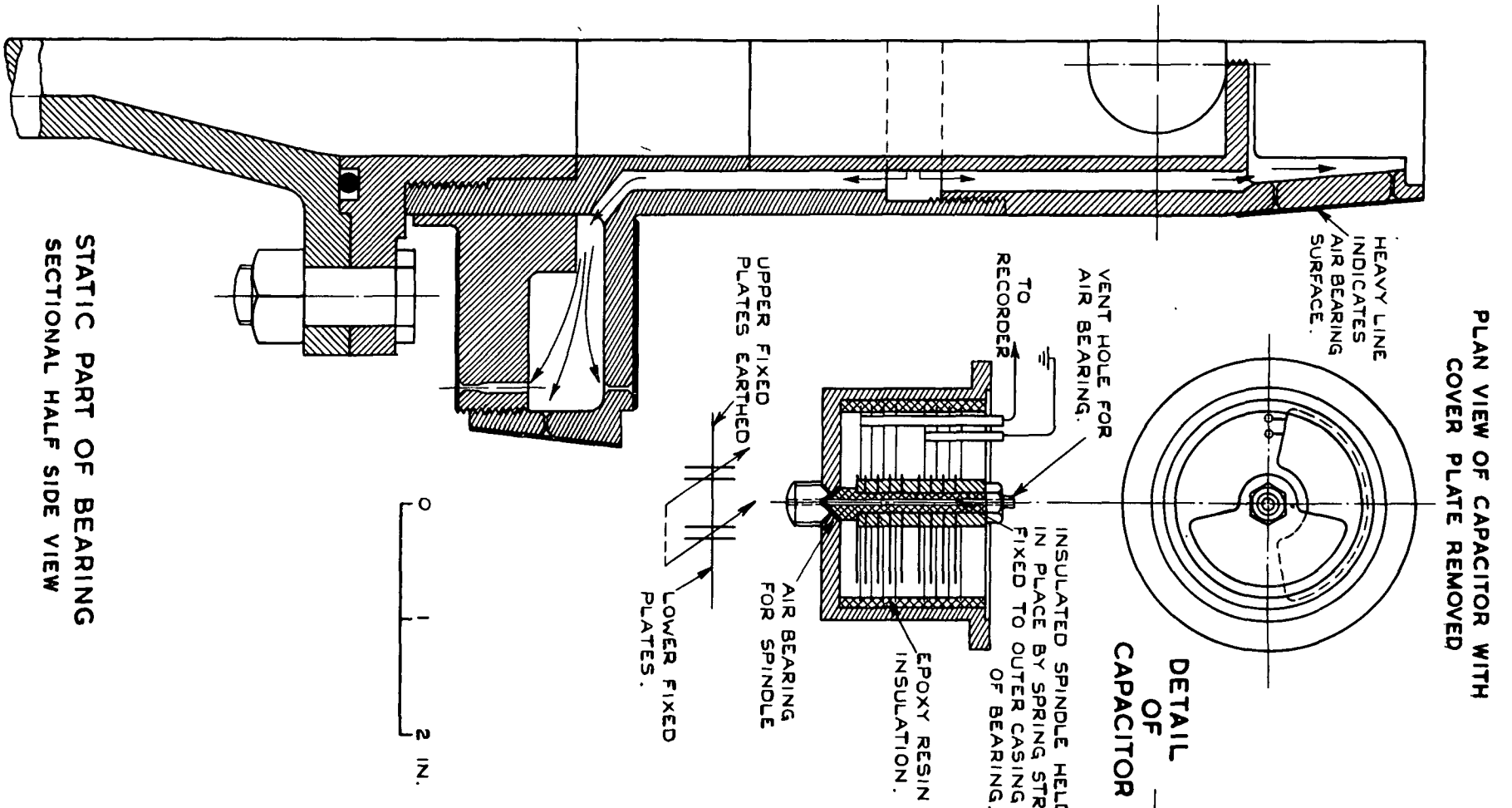


FIG. 1. ORIGINAL BEARING DESIGN.

FIG. 2. FINAL BEARING DESIGN.

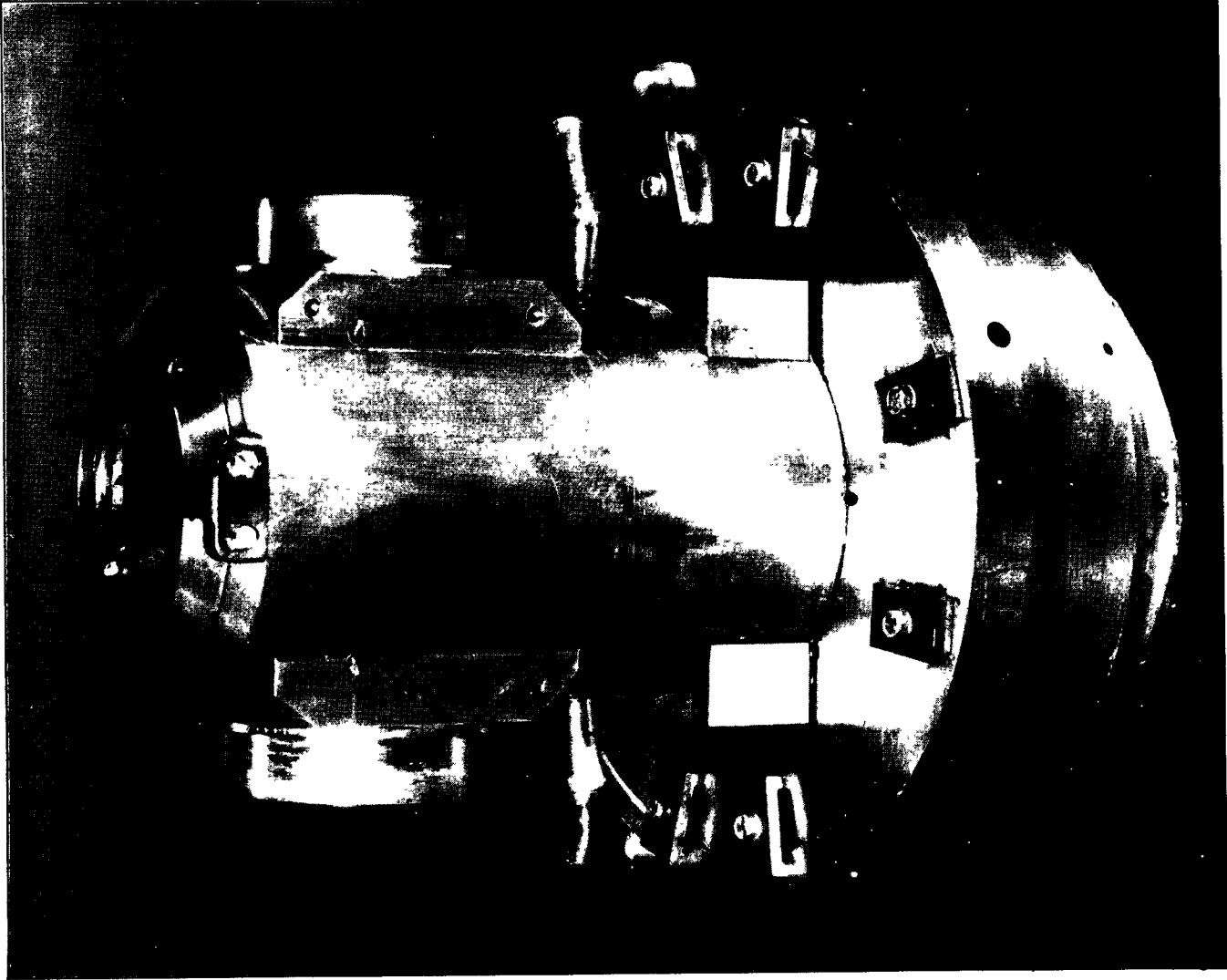


FIG.3. MODIFIED BEARING ASSEMBLY

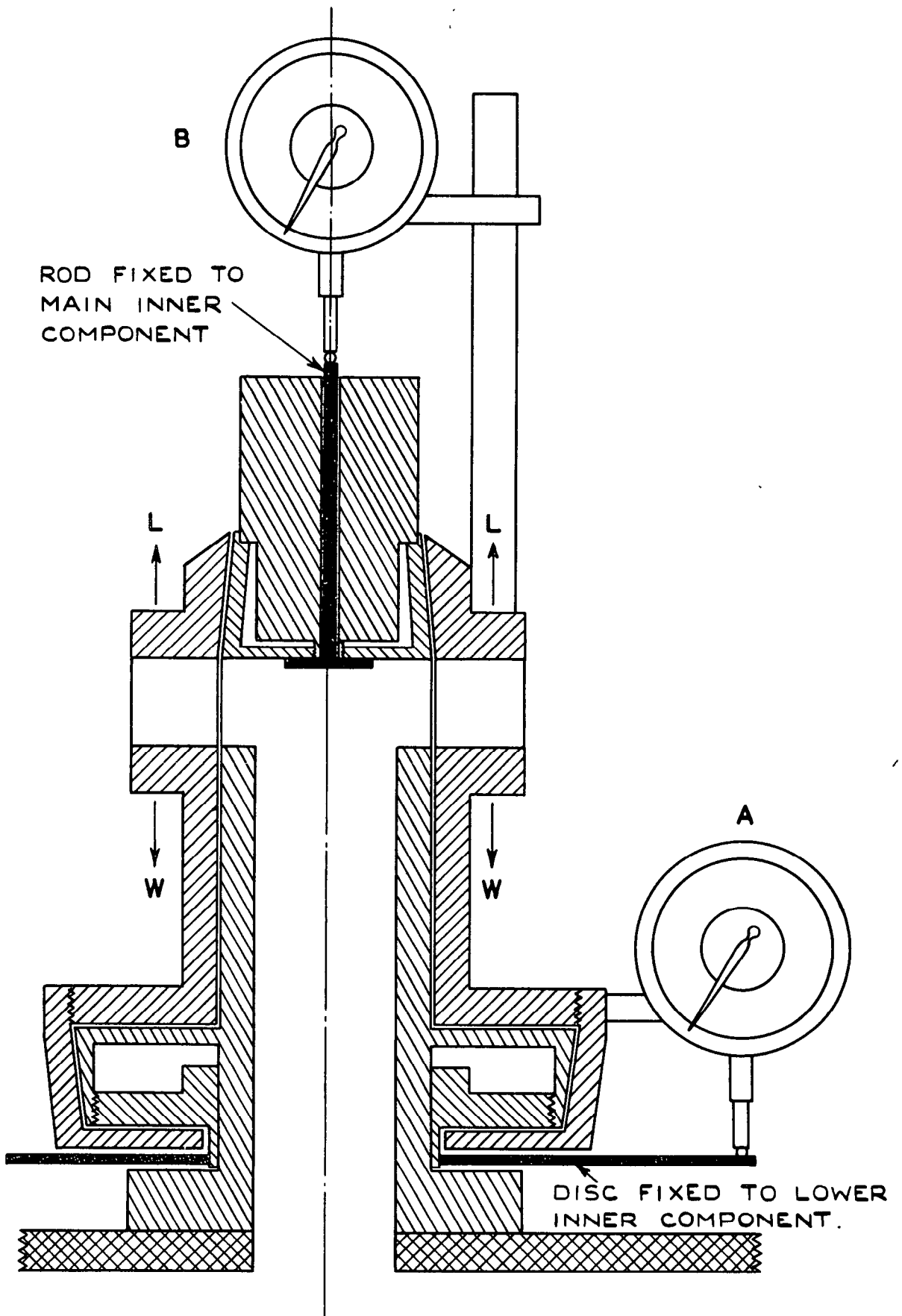


FIG. 4. METHOD OF GAP MEASUREMENT FOR HORIZONTAL BEARINGS.

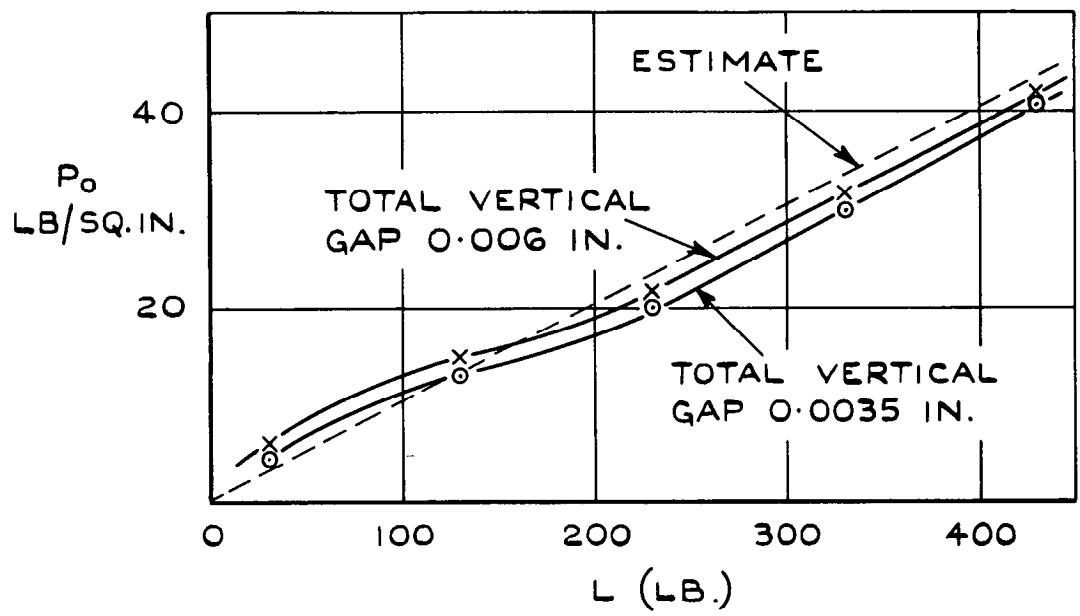
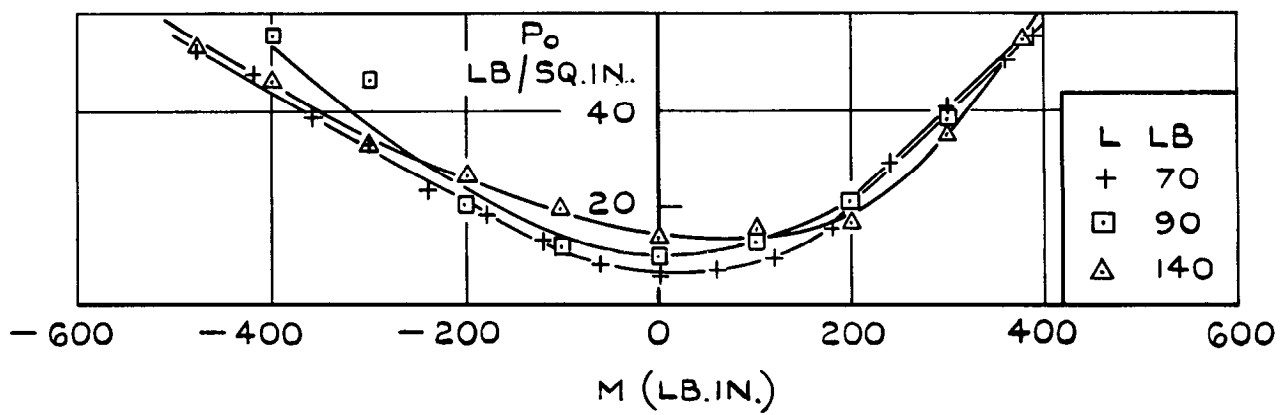
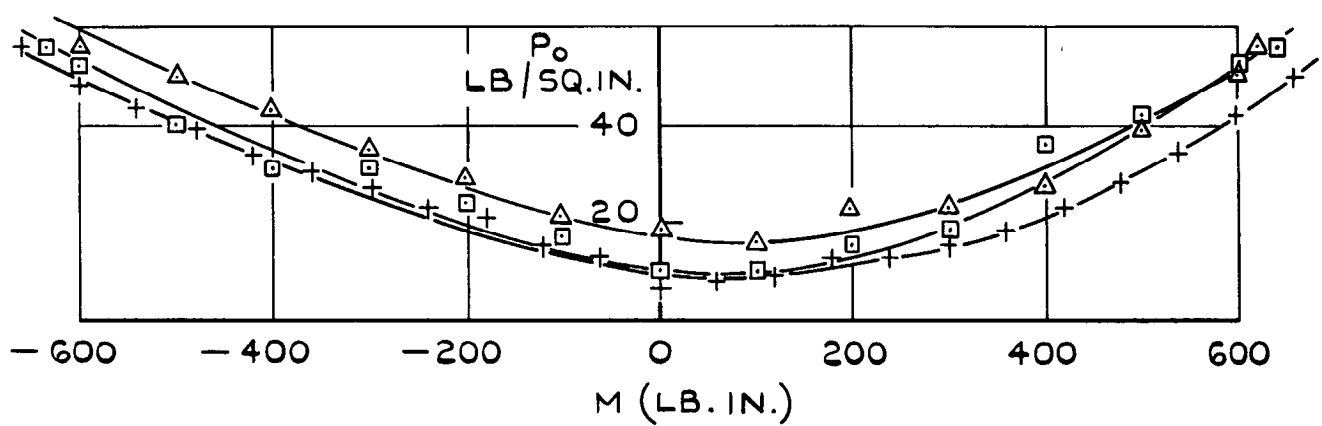


FIG. 5. LIFT CAPACITY OF BEARING.

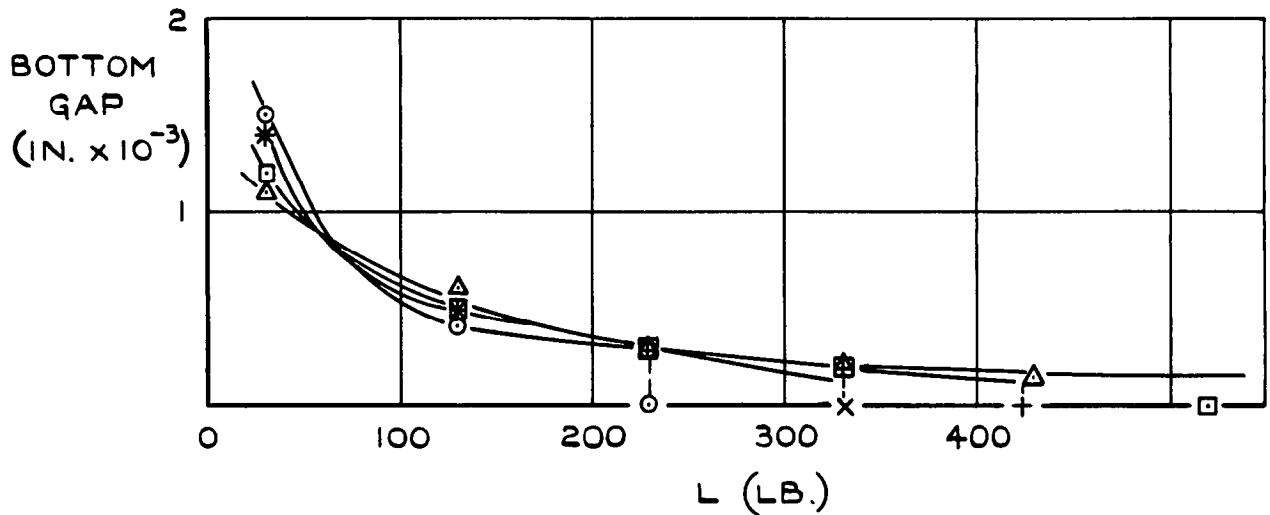


(a) TOTAL VERTICAL GAP = 0.006 IN.

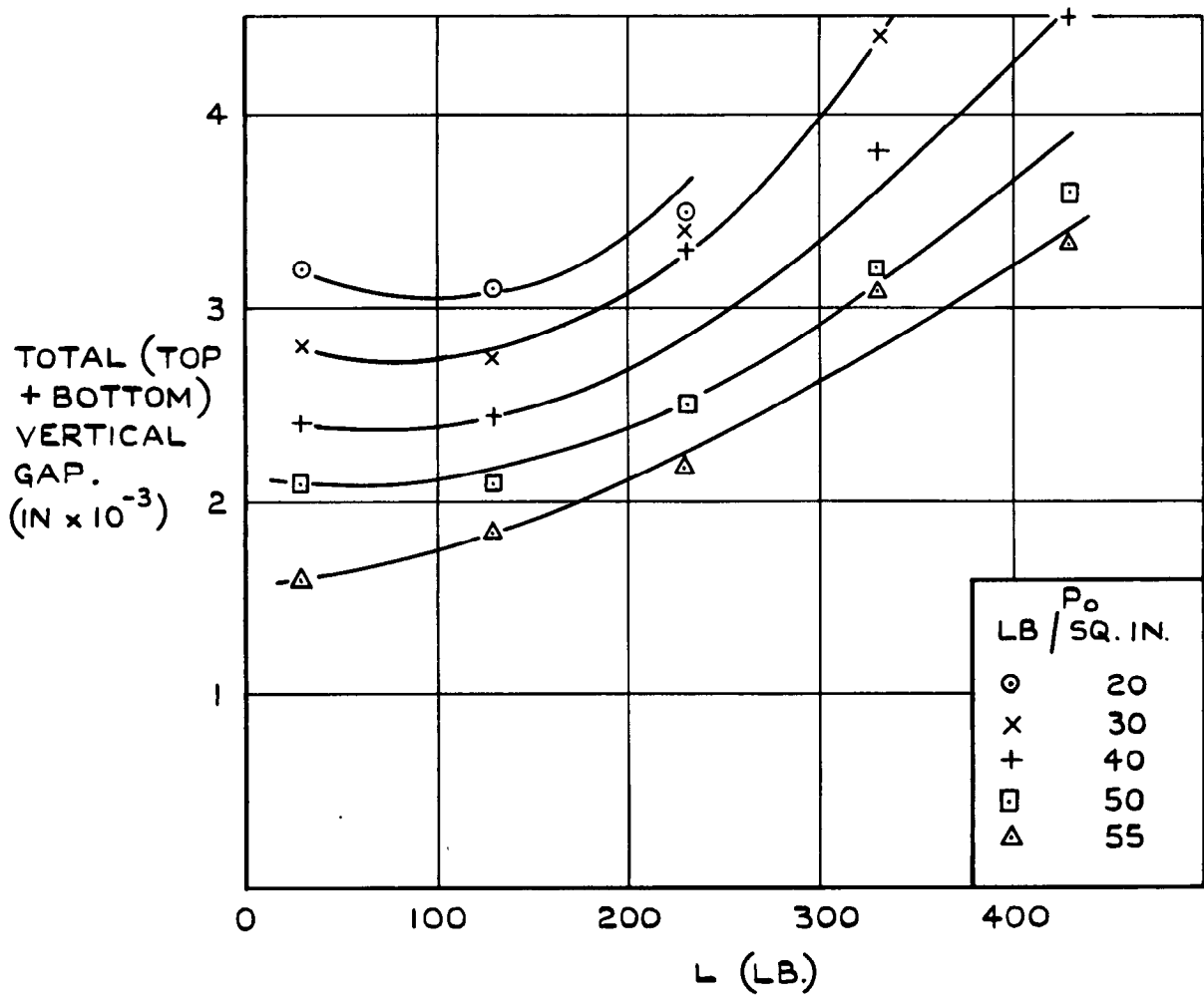


(b) TOTAL VERTICAL GAP = 0.0035 IN.

FIG. 6. COMBINED LIFT AND PITCHING-MOMENT CAPACITY OF BEARING.



(a) VARIATION OF LOWER GAP WITH LIFT LOAD.



(b) VARIATION OF TOTAL (TOP + BOTTOM) GAP WITH LIFT LOAD.

FIG. 7. EFFECT OF LIFT LOAD ON HORIZONTAL BEARING SURFACE GAPS.(TOTAL GAP INITIALLY SET AT 0.0035 IN.)

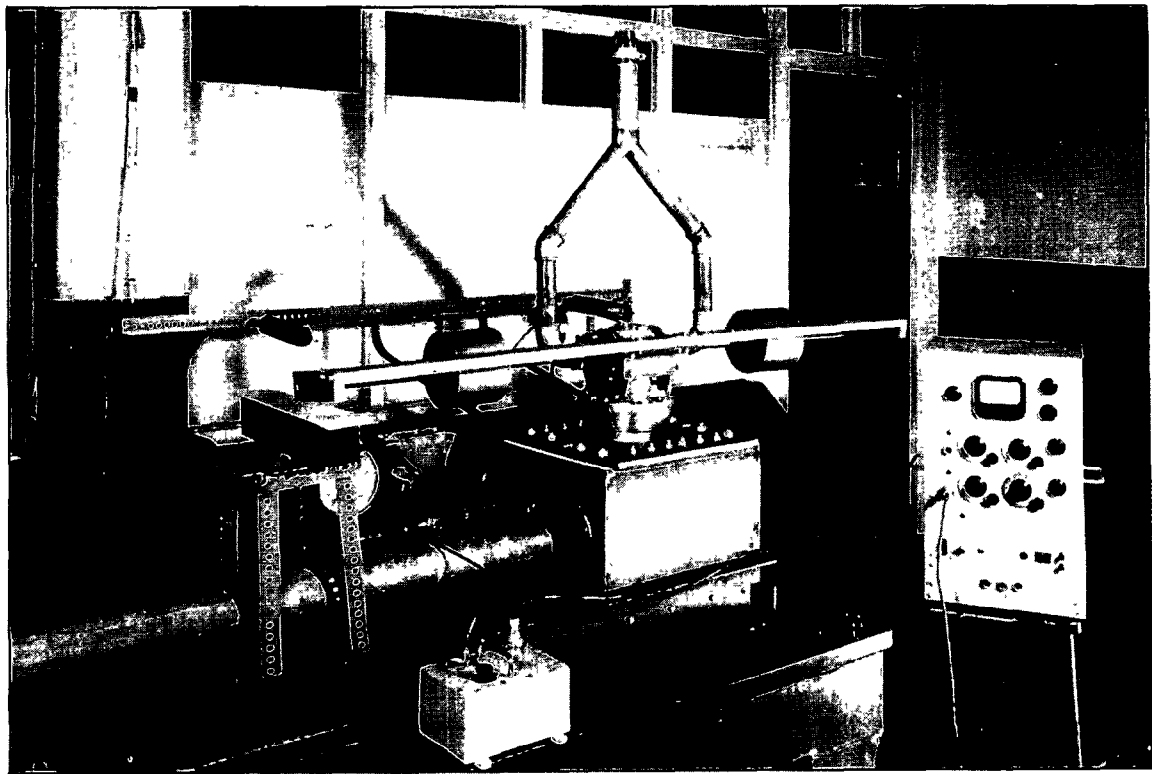


FIG.8. ARRANGEMENT FOR THE MEASUREMENT OF INTERNAL OSCILLATORY DAMPING

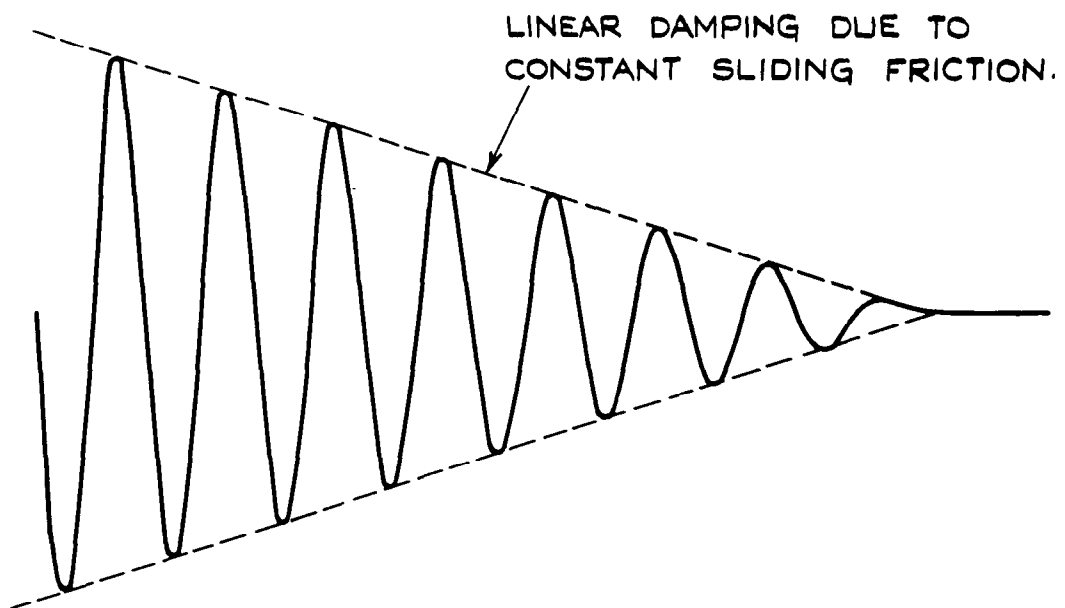


FIG.9. TYPICAL TRACE OF OSCILLATORY DAMPING WITH THE BEARING OVERLOADED

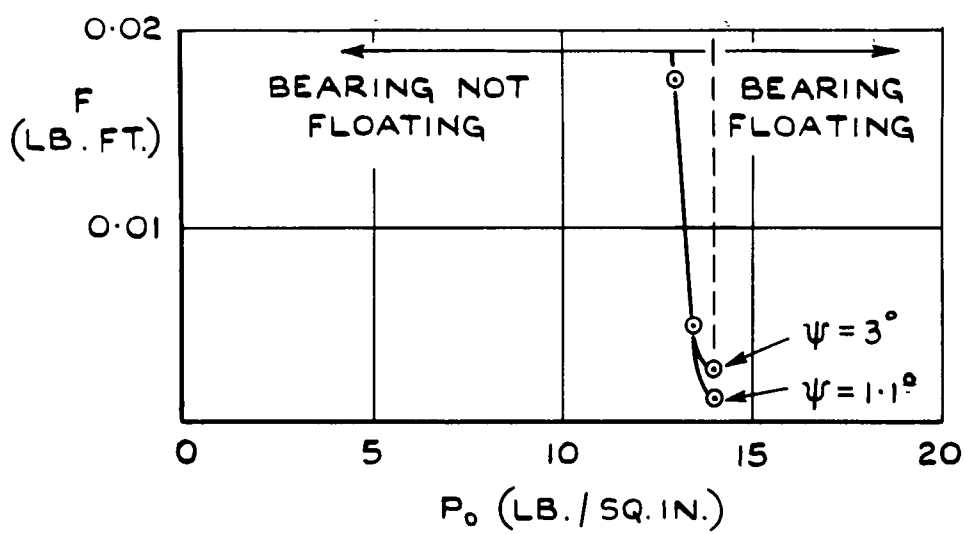


FIG. 10. CHANGE IN EQUIVALENT SLIDING FRICTION AS BEARING STARTS TO FLOAT. $L = -110$ LB.

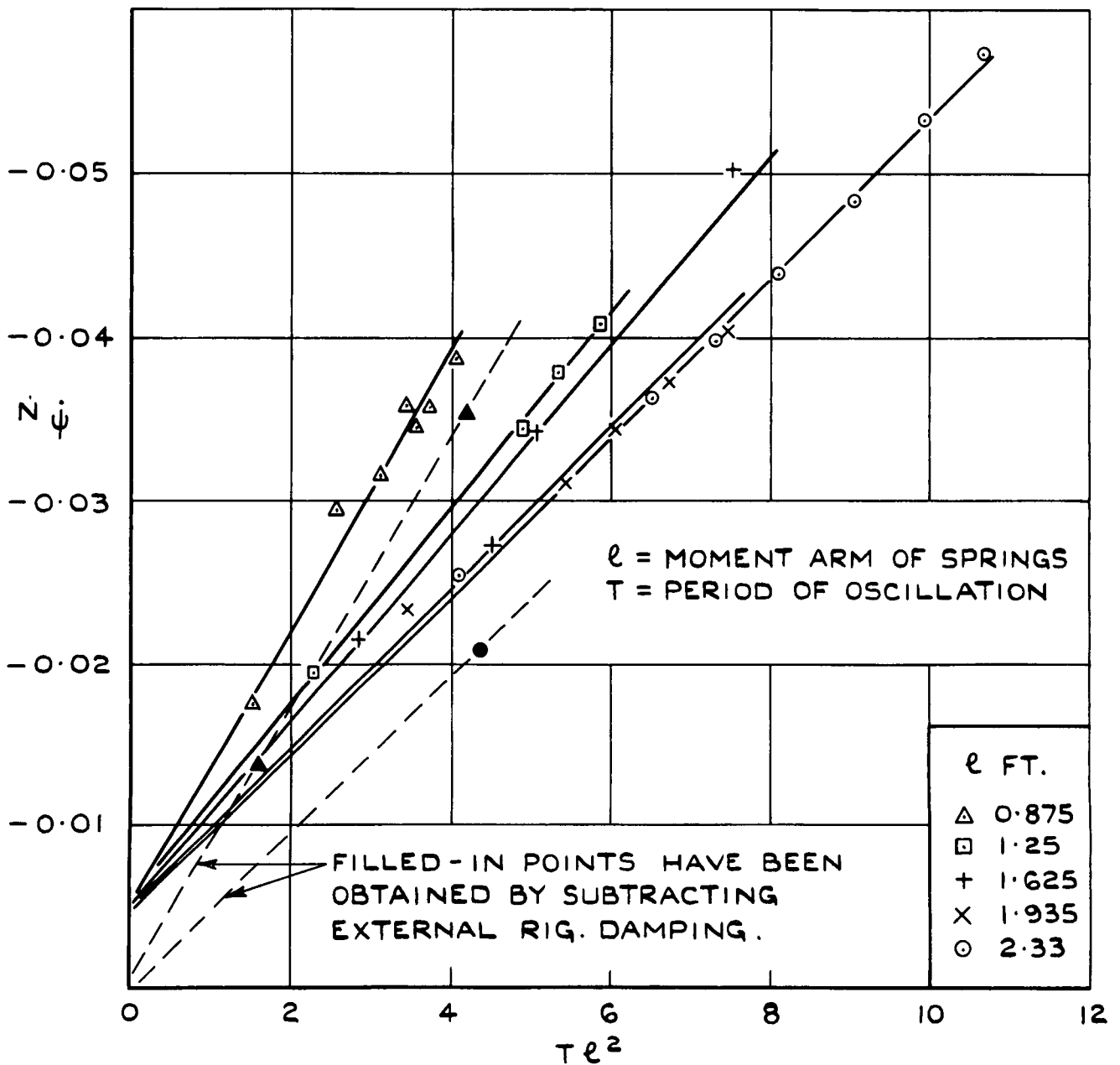


FIG. 11. VARIATION OF $N\dot{\psi}$ WITH SPRING HYSTERESIS PARAMETER, $T\ell^2$

A.R.C. C.P. No. 796

533.6.071.3 :
533.652.6 :
533.694.6 :
533.6.013.154

THE DESIGN AND DEVELOPMENT OF AN AIR-BEARING FOR THE MEASUREMENT OF DAMPING IN YAW ON A JET-BLOWING MODEL. Cox, A.P. April 1964

This Note describes the design and development of an air-bearing support assembly, for damped oscillation measurements of yaw damping derivatives on V./S.T.O.L. blowing models, commencing with a jet-flap model. The bearing, fitted within the fuselage, allowed freedom in yaw, but supported all the other forces and moments. Typically, with a bearing air supply of 0.07 lb/sec at 60 p.s.i.g., a vertical load of 400 lb could be sustained, or a pitching-moment of 650 lb in. with the vertical load reduced to 150 lb. From measurements of the overall rig damping rate, the internal damping of the bearing was determined by allowing for the contributions from spring hysteresis loss and external aerodynamic loads.

(Over)

A.R.C. C.P. No. 796

533.6.071.3 :
533.652.6 :
533.694.6 :
533.6.013.154

THE DESIGN AND DEVELOPMENT OF AN AIR-BEARING FOR THE MEASUREMENT OF DAMPING IN YAW ON A JET-BLOWING MODEL. Cox, A.P. April 1964

This Note describes the design and development of an air-bearing support assembly, for damped oscillation measurements of yaw damping derivatives on V./S.T.O.L. blowing models, commencing with a jet-flap model. The bearing, fitted within the fuselage, allowed freedom in yaw, but supported all the other forces and moments. Typically, with a bearing air supply of 0.07 lb/sec at 60 p.s.i.g., a vertical load of 400 lb could be sustained, or a pitching-moment of 650 lb in. with the vertical load reduced to 150 lb. From measurements of the overall rig damping rate, the internal damping of the bearing was determined by allowing for the contributions from spring hysteresis loss and external aerodynamic loads.

(Over)

A.R.C. C.P. No. 796

533.6.071.3 :
533.652.6 :
533.694.6 :
533.6.013.154

THE DESIGN AND DEVELOPMENT OF AN AIR-BEARING FOR THE MEASUREMENT OF DAMPING IN YAW ON A JET-BLOWING MODEL. Cox, A.P. April 1964

This Note describes the design and development of an air-bearing support assembly, for damped oscillation measurements of yaw damping derivatives on V./S.T.O.L. blowing models, commencing with a jet-flap model. The bearing, fitted within the fuselage, allowed freedom in yaw, but supported all the other forces and moments. Typically, with a bearing air supply of 0.07 lb/sec at 60 p.s.i.g., a vertical load of 400 lb could be sustained, or a pitching-moment of 650 lb in. with the vertical load reduced to 150 lb. From measurements of the overall rig damping rate, the internal damping of the bearing was determined by allowing for the contributions from spring hysteresis loss and external aerodynamic loads.

(Over)

The internal damping of the bearing, which was unaffected by the transmission of the simulated wing airflow (amounting to 2 lb/sec at 15 p.s.i.g.), was found to be negligible as long as the bearing capacity was not exceeded.

The internal damping of the bearing, which was unaffected by the transmission of the simulated wing airflow (amounting to 2 lb/sec at 15 p.s.i.g.), was found to be negligible as long as the bearing capacity was not exceeded.

The internal damping of the bearing, which was unaffected by the transmission of the simulated wing airflow (amounting to 2 lb/sec at 15 p.s.i.g.), was found to be negligible as long as the bearing capacity was not exceeded.

C.P. No. 796

© *Crown Copyright 1965*

Published by
HER MAJESTY'S STATIONERY OFFICE

To be purchased from
York House, Kingsway, London w.c.2
423 Oxford Street, London w.1
13A Castle Street, Edinburgh 2
109 St. Mary Street, Cardiff
39 King Street, Manchester 2
50 Fairfax Street, Bristol 1
35 Smallbrook, Ringway, Birmingham 5
80 Chichester Street, Belfast 1
or through any bookseller

C.P. No. 796

S.O. CODE No. 23-9015-96